AIP | Applied Physics Letters

The A-site Li+ driven orthorhombic-tetragonal ferroelectric phase transition and evolving local structures in (Na,K)(Nb,Sb)O3-LiTaO3 lead-free ceramics

Jian Fu and Ruzhong Zuo

Citation: Appl. Phys. Lett. **102**, 122902 (2013); doi: 10.1063/1.4798830
View online: http://dx.doi.org/10.1063/1.4798830
View Table of Contents: http://apl.aip.org/resource/1/APPLAB/v102/i12
Published by the American Institute of Physics.

The A-site Li^+ driven orthorhombic-tetragonal ferroelectric phase transition and evolving local structures in (Na,K)(Nb,Sb)O_3-$LiTaO_3$ lead-free ceramics

Jian Fu and Ruzhong Zuo[a)]
Institute of Electro Ceramics and Devices, School of Materials Science and Engineering, Hefei University of Technology, Hefei 230009, People's Republic of China

(Received 16 November 2012; accepted 18 March 2013; published online 27 March 2013)

Synchrotron x-ray diffraction and absorption fine structure and Raman spectra on (Na,K)(Nb,Sb)O_3-$LiTaO_3$ ceramics suggested that the compositionally induced orthorhombic to tetragonal (O-T) ferroelectric phase transition is dominantly driven by A-site Li^+ ions with a large [001] off centering, while B-site Nb atoms are only localized near their average positions of the NbO_6 octahedra between O and T phases. The Nb-O octahedra distort over the phase transition by adjusting their positions and orientations. The continuous change of lattice constants b_o and a_t across the phase boundary would facilitate the O-T phase transition through a jump of polar axis from pseudocubic [101] to [001].
 [http://dx.doi.org/10.1063/1.4798830]

The crystal structural transformation owing to a change of the composition in ferroelectric materials has been extensively studied in recent years because the phase instabilities at the phase boundary, which separates one polar phase from another polar phase or nonpolar phase,[1] tends to induce outstanding dielectric and piezoelectric properties. In typical perovskite solid solutions such as Pb(Zr,Ti)O_3 (PZT),[2] the best piezoelectric properties were found out near a morphotropic phase boundary (MPB) between ferroelectric tetragonal (T) phase and ferroelectric rhombohedral (R) phase. In comparison with MPB, a polymorphic phase boundary (PPB) was recognized in (Na,K)NbO_3 (NKN) based lead-free piezoelectric materials,[3,4] near which the optimum piezoelectric properties could also be obtained particularly because of the coexistence of orthorhombic (O) and T ferroelectric phases.

Saito *et al.* reported in 2004 that the Li, Ta, and Sb modified NKN ceramics own excellent piezoelectric properties close to the O and T phase coexistence zone.[5] Their dielectric and piezoelectric properties were further enhanced by optimizing the relative content of Li, Ta, and Sb dopants.[4] The enhanced piezoelectric properties in the vicinity of the O-T PPB were ascribed either to the presence of nanodomains[5] or to electric-field induced phase instability.[6,7] Recently, the local structure transition in NKN based compositions was studied as a function of temperature by means of x-ray absorption technique.[8,9] As known, the formation of the phase boundary (either MBP or PPB) was not caused by the variation of the temperature rather than the composition. How the polymorphic ferroelectric phase transformation evolves from O symmetry to T symmetry with slightly changing the composition is still not clear. A lot of studies have been devoted to the phase structure transition near R-T MPB for commercially used PZT ceramics.[10,11] It would be of much interest to know what is the difference in the phase transition behavior for both typical piezoelectric systems.

In the present work, the composition-induced O to T ferroelectric phase transition process in $LiTaO_3$ modified (Na,K)(Nb,Sb)O_3 lead-free ceramics was elucidated by means of Raman spectroscopy and high-resolution synchrotron x-ray diffraction. The local structure evolution during the phase transition was refined by extended x-ray absorption fine structure (EXAFS). These measurements were expected to point out how O symmetry gradually transforms into T symmetry with changing the composition from the crystallographic point of view and clarify what is the mechanism of the phase transition from the local structural change in a perovskite unit cell.

Lead-free $(Na_{0.52}K_{0.48-x})(Nb_{0.92-x}Sb_{0.08})O_3$-$xLiTaO_3$ (NKNS-xLT) ($0.01 \leq x \leq 0.07$) ceramics were prepared by a conventional solid-state reaction method as reported previously.[4] Raman spectra were collected at room temperature using an inVia Raman microscope (Renishaw, Gloucestershire, UK) with a backscattering configuration. The excitation laser was irradiated from the YAG laser with a wavelength of 532 nm and an output power of 10 mV. High-resolution synchrotron x-ray powder diffraction measurements were taken at beam line 14B1 at Shanghai Synchrotron Radiation Facility (SSRF). This beam line provides a monochromatic incident beam with a wavelength close to 0.6887 Å (18 keV) from a Si(111) double-crystal monochromator. Coupled θ-2θ scans were performed over selected angular regions about the pseudocubic reflections (200), (220), and (222) with a 2θ step interval of 0.005°. The x-ray absorption spectra of the Nb K-edge (18.986 keV) were measured at beam line 14W1 of SSRF by using a Si(111) double-crystal monochromator. Before the x-ray absorption measurements, the as-prepared ceramic powders were mixed with boron nitride (BN) powders (the mass ratio between the ceramic powder and the BN powder is 3:7) and then pressed into homogeneous self-supporting pellets. Due to the high stability and the low absorption coefficient of BN, it cannot change the crystallographic phase structure and the absorption data in XAFS. The EXAFS of Nb K-edge spectra was analyzed with IFEFFIT package.[12]

Figure 1 shows the synchrotron powder x-ray diffraction patterns of (200), (220), and (222) pseudocubic reflections

[a)]Author to whom correspondence should be addressed. Electronic mail: piezolab@hfut.edu.cn. Tel.: 86-551-2905285. Fax: 0086-551-2905285.

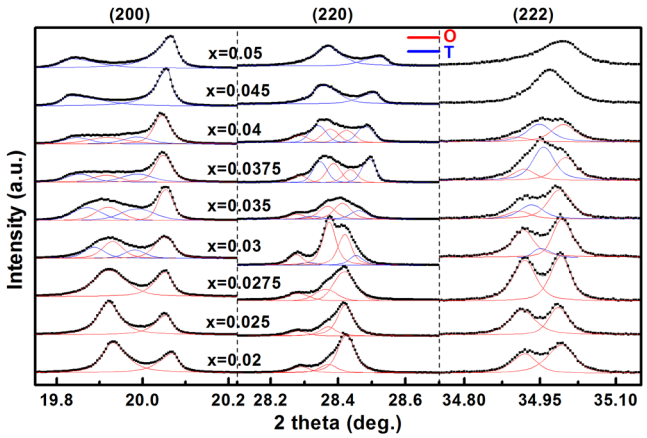

FIG. 1. Evolution of the synchrotron diffraction profiles of the (200), (220), and (222) pseudocubic reflections for lead-free NKNS-xLT ceramics with different LT contents.

for NKNS-xLT ceramic powders. The fitting analysis of the diffraction peak profiles was carried out by using pseudo-Voigt peak shape function. The symmetry of the samples can be well established from the peak splitting and the relative intensity of these reflection lines. An O symmetry can be resolved for samples with $0.02 \leq x \leq 0.03$, as characterized by two doublets at pseudocubic (200) and (222) peaks ((202)/(020) doublet and (024)/(420) doublet, respectively) and a triplet at (220) peaks ((004)/(400)/(222) peaks). These features look similar to the O phase observed in $BaTiO_3$ and $Pb(Zn_{1/3}Nb_{2/3})$-$PbTiO_3$.[10,13] As x is beyond 0.04, the compositions clearly show a T phase, demonstrated by the single (222) reflection, and two doublets (200)/(002) and (202)/(220) with a stronger outer line and inner line, respectively. By comparison, the compositions with $x = 0.03$–0.04 can be considered to consist of the mixture of the O and T phases. A monoclinic symmetry was found in $LiNbO_3$ modified NKN (NKN-LN) ceramics,[14] probably because the different manner of ionic substitution resulted in the variation of the Na/K ratio between NKN-LN and NKNS-xLT ceramics.

Figure 2 shows the variation of the lattice parameters with changing the LT content. The lattice parameters of O symmetry are determined by the relationship between the unit cell of O symmetry and the subcell of monoclinic

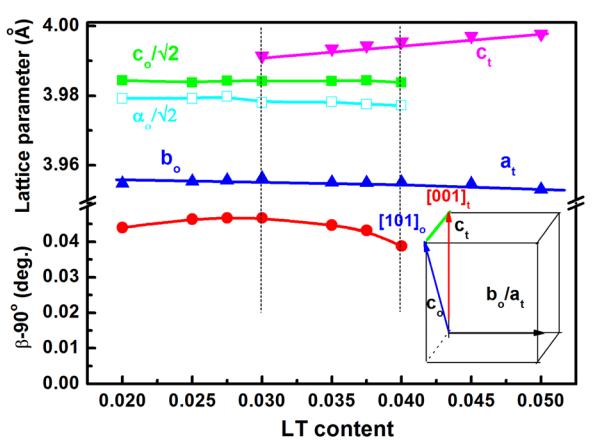

FIG. 2. Composition dependence of the lattice parameters of the NKNS-xLT ceramics in the vicinity of PPB at room temperature and the inset is the sketch of the crystallographic relationship between O and T phase.

symmetry.[15,16] It can be seen that the lattice parameters in the O phase zone only slightly change. As $x \geq 0.03$, a T symmetry starts to appear in the matrix of the O symmetry, and its c_t/a_t ratio gradually increases from 1.009 at $x = 0.03$ to 1.0114 at $x = 0.05$. Interestingly, the variation between b_o and a_t is continuous as the composition is across the O-T coexistence zone. For O and T perovskite unit cells, these two axes (b_o and a_t) are perpendicular to their respective polar axes, as can be seen from the inset of Fig. 2. However, the polar axis jumps from pseudocubic [101] to [001] owing to a discontinuous change between c_o and c_t, as a phase transition from O to T occurs. Based on the conformal miniaturization of stress-accommodating tetragonal domains under the condition of low domain-wall energy density,[17] a similar phenomenon was observed in Pb-based perovskite materials where the lattice parameters between these two phases were found to obey an invariance condition of $b_o = a_t$. For the same reason, it seems that there should exist nanoscaled microdomains with low domain-wall energy in currently studied compositions.[5] In addition, it is also found that β angle, which is defined as the angle of the monoclinic subcell in the O phase zone, is less than 90.05°. This value is much lower than that in other NKN-based materials.[14] The low domain-wall energy and low β angle difference between O (or monoclinic subcell) and T phases would result in a very-low-energy barrier in NKNS-xLT materials as the composition lies in the vicinity of PPB, such that the crystal structure transformation from O (Amm2) to T (P4mm) phases can be relatively easily induced by composition.

Raman spectroscopy was used in this work to detect the local ionic configuration within a short range as a complement to the XRD results that generally disclose a long-range average structure. Figure 3(a) shows the typical Raman spectra of NKNS-xLT ceramics. A group theoretical analysis led to 12 Raman active modes ($4A_1 + 4B_1 + 3B_2 + A_2$) for the NKN with Amm2 space group, while the NKN with P4mm space group has 8 Raman active modes ($3A_1 + B_1 + 4E$).[18] The observed vibrations in Fig. 3(a) can be separated into translational modes of the isolated A site cations and internal modes of the coordination octahedra (ν_1, ν_2, ν_3, ν_4, ν_5, and ν_6). In these modes, the ν_1 ($\sim 600\,cm^{-1}$) mode, which has been assigned to the lattice vibration of A_1 mode, is closely related to the strength and length of the B-O bond, and the ν_5 ($\sim 250\,cm^{-1}$) mode, which has been assigned to the modes of $A_1 + B_1 + B_2$ (O symmetry) or $A_1 + E$ (T symmetry),[18] represents a double-degenerate O-B-O stretching vibration, where the oxygen is situated along the polarization direction, and a triple-degenerate O-B-O bending vibration where the oxygen is located in the plane perpendicular to the polarization direction, as sketched in the inset of Fig. 3(b). These two modes were detected as relatively strong scattering intensities compared to other vibrational modes. In addition, these two modes show an obvious peak shift to higher frequency with increasing the LT content, demonstrating that the substitution of Li and Ta ions can induce the lattice distortion including both the variation of the distance between the B site ion and its coordinated oxygen, and the change of the O-B-O angles. From the aforementioned discussion, it can be inferred that an abrupt change of the ν_1 and ν_5 modes near $x = 0.03$ would be correlated to the emergence of a T

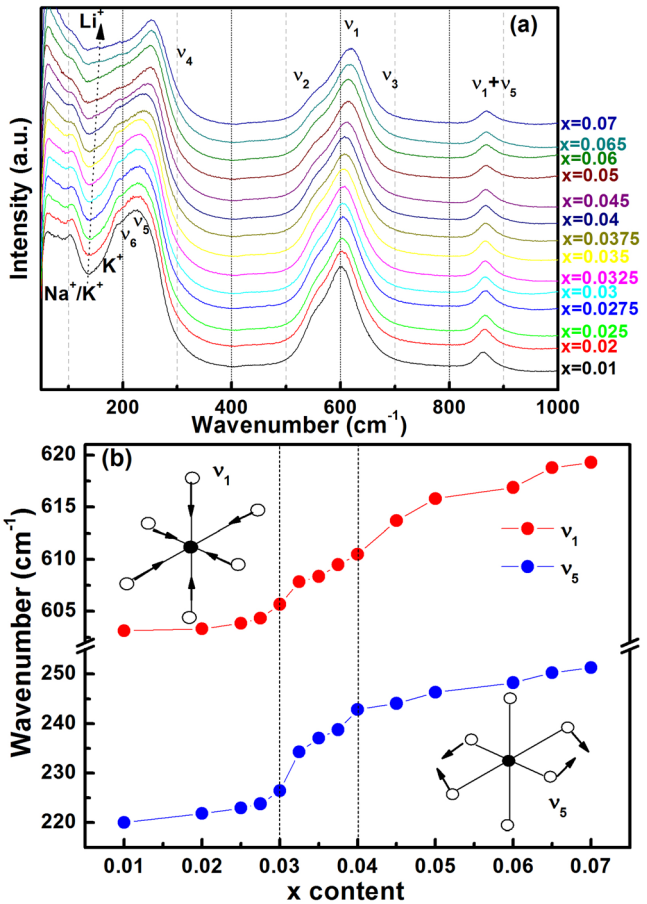

FIG. 3. (a) Raman spectra of NKNS-xLT ceramics as a function of various LT contents from x = 0.01 to x = 0.07 measured at room temperature. (b) Composition dependence of the frequencies of Raman peaks for NKNS-xLT ceramics at room temperature.

phase, which is accompanied by a discontinuous change of the polar axis from [101] for O phase to [001] for T phase (i.e., a discontinuous change of the B-O bond) and a distortion of the O-B-O angle. As the x value is above 0.03, a distinct peak shift of the ν_1 and ν_5 modes should be ascribed to the increase of the tetragonality (c/a ratio) (Fig. 2) as well as the Curie temperature.[4] However, the composition induced O-T phase transition in this work seems to be related to the addition of A-site Li ions instead of B-site Ta ions if the translational modes of alkaline cations were taken into account.

As can be seen from Fig. 3(a), there are three vibration modes below 200 cm^{-1}. The two modes at ~105 cm^{-1} and ~190 cm^{-1} can be assigned to Na-O/K-O vibrations,[19] and the mode at ~150 cm^{-1} should correspond to the vibration involving the Li-O bond. One can see that with an increase of x, the intensity of the translational modes of Na^+/K^+ cations starts to decrease. At the same time, the translational mode of the Li^+ cation emerges, as manifested by the fact that the valley near 150 cm^{-1} humps gradually and becomes a broad scattering peak as x is beyond 0.04. It is worthy of note that the Li^+ content is much smaller than the amount of Na^+ and K^+ cations in the studied composition range. Nevertheless, the mode near 150 cm^{-1} obviously shifts to higher frequencies with increasing the Li^+ content. By comparison, no Raman shift can be seen in the modes associated with the Na-O/K-O bonds. It is indicated that the formation of the T phase and the increase of the tetragonality should be mainly caused by A-site Li^+ ions rather than A-site Na^+/K^+ ions and B-site Ta ions. Actually, the substitution of Ta^{5+} for Nb^{5+} tends to decrease the T_c value of the system and weaken the anisotropy of the unit cell. Most importantly, it has been found that TaO_6 octahedron is not distorted in alkaline niobate tantalate,[20] which hints that the addition of Ta in alkaline niobate should favor the pseudocubic/cubic phase instead of T phase. It is thus believed that Li^+ with a small atomic radius plays an important role in the O-T phase transition as well as the change of the Nb-O octahedron distortion during the O-T phase transition. That is to say, smaller A-site ions tend to restrain the rotational instabilities owing to the frustration between large and small A-site ions and provide A-site driven rather than B-site driven ferroelectricity.

Figure 4 shows the normalized Nb K-edge XAFS spectra at room temperature of NKNS-xLT samples selected in the vicinity of PPB. To obtain the information about the composition dependent local structure evolution in NKNS-xLT ceramics, the Fourier transforms of the EXAFS spectra of the k^3-weighted K-edges exhibiting the contribution of photoelectron scattering on nearest neighbors around Nb in NKNS-xLT samples are shown in the inset of Fig. 4, where R refers to the distribution of neighbors in the various shells around Nb. These spectra are characterized by the three obvious shells consisting of BO_6 octahedra and isolated A-site ions. In the R range from 1.0 and 4.0 Å, the first two peaks near R = 1–2 Å correspond to the octahedral O environment. The splitting of the oxygen shell is due to the displacement of the oxygen shell relative to the Nb. This shows that two types of Nb-O distance exist in the O phase as well as in the T phase. The next peaks near R = 2–3 Å are due to the first eight K/Na/Li neighbors. The strongest peak of the Nb atoms in the six closest octahedra near R = 3.5 Å is observed. It is noted that all the moduli curves of the Fourier transforms are not phase corrected, and the actual bond length may be longer than, ca., 0.2–0.5 Å. In order to obtain quantitative structural information, we fitted the first shell region by assuming the coexistence of O and T phases, where the content of the T phase was set as F_T ($0 \le F_T \le 1$).

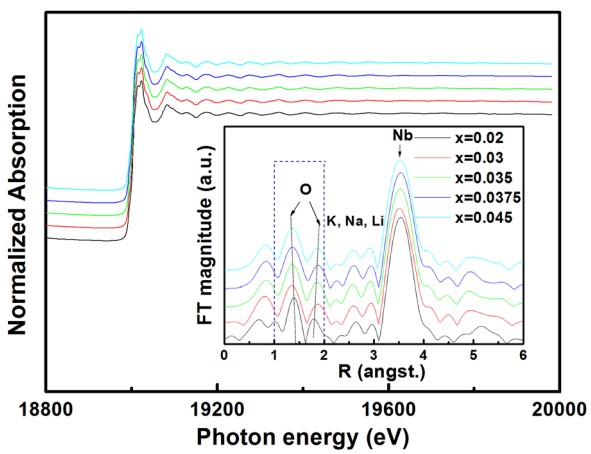

FIG. 4. The normalized Nb K-edge XAFS spectra of selected NKNS-xLT samples as indicated. The inset refers to the Fourier transforms of the EXAFS spectra.

TABLE I. Parameters of the first coordination shell around Nb atom in NKNS-xLT powders. N is a coordination number of a subshell, R is the Nb-O distance for the subshell, and σ^2 is a corresponding Debye-Waller factor.

Sample	Phase	F_T	Bond	N	R (Å)	σ^2 (Å^2)
x = 0.02	O	0.0	Nb-O	3	1.890	0.0062
			Nb-O	3	2.093	0.0067
x = 0.03	O	0.51	Nb-O	3	1.891	0.0067
			Nb-O	3	2.095	0.0069
	T		Nb-O	3	1.892	0.0045
			Nb-O	3	2.101	0.0047
x = 0.035	O	0.63	Nb-O	3	1.891	0.0073
			Nb-O	3	2.096	0.0077
	T		Nb-O	3	1.892	0.0048
			Nb-O	3	2.102	0.0051
x = 0.0375	O	0.68	Nb-O	3	1.891	0.0082
			Nb-O	3	2.096	0.0086
	T		Nb-O	3	1.893	0.0055
			Nb-O	3	2.104	0.0058
x = 0.045	T	1.00	Nb-O	3	1.893	0.0058
			Nb-O	3	2.107	0.0060

The extracted structural parameters of the first shell fitting for NKNS-xLT are presented in Table I. With increasing the LT content, the splitting of the oxygen shell increases, characterized by the significant shrinkage and expansion of the lengths of small and large Nb-O bonds, respectively, meaning that the addition of LT induces an increase of the anisotropy of the unit cells. In comparison to the x-ray diffraction data, a continuous change in the Nb-O distance can be observed in the range of x = 0.02–0.045, meaning that the Nb atoms should be localized near their average positions of NO_6 octahedra between O and T phases. The results also indicate that the composition induced O-T phase transition does not affect the inside of the octahedron but their relative positions and orientations, similar to the temperature induced O-T phase transition.[9] In addition, the Debye-Waller factor σ^2 in the T phase is much smaller than that in the O phase, which is consistent with the fact that the T phase in NKNS-xLT is relatively energetically favored by the addition of Li.[21] Unfortunately, the fitting in the second and third shell regions might be too complicated due to a great number of free parameters.

In summary, the phase transformation mechanism from O to T symmetry in lead-free NKNS-xLT ceramics was explored by means of Raman spectra and synchrotron x-ray diffraction and absorption techniques. The results indicate that the composition induced crystal structure transition in NKNS-xLT can be completed through a jump of polar axis from pseudocubic [101] to [001], in which the T phase should be dominantly induced by A-site smaller Li ions with a large off centering along [001] direction. However, the B-site Nb atoms are only localized near their average positions of the NbO_6 octahedra between O and T phases. The Nb-O octahedra distortion changes over the phase transition by adjusting their positions and orientations. The continuous change of lattice constants b_o and a_t across the phase boundary would facilitate the O-T phase transition through a jump of polar axis from pseudocubic [101] to [001].

The authors would like to thank Shanghai Synchrotron Radiation Source for use of the synchrotron radiation facilities and kind help from Professor J. Z. Jiang of Zhejiang University. Financial support from the Natural Science Foundation Anhui Province (Grant No. 1108085J14) and the National Natural Science Foundation of China (Grant No. 51272060) is gratefully acknowledged.

[1]D. Damjanovic, Appl. Phys. Lett. **97**, 062906 (2010).
[2]B. Jaffe, W. R. Cook, and H. Jaffe, *Piezoelectric Ceramics* (Academic Press, New York, 1971).
[3]Y. Saito, H. Takao, T. Tani, T. Nonoyama, K. Takatori, T. Homma, T. Nagaya, and M. Nakamura, Nature (London) **432**, 84 (2004).
[4]R. Z. Zuo, J. Fu, and D. Y. Lv, J. Am. Ceram. Soc. **92**, 283 (2009).
[5]J. Fu, R. Z. Zuo, and Z. K. Xu, Appl. Phys. Lett. **99**, 062901 (2011).
[6]E. K. Akdogan, K. Kerman, M. Abazari, and A. Safari, Appl. Phys. Lett. **92**, 112908 (2008).
[7]R. Z. Zuo, J. Fu, G. Z. Yin, X. L. Li, and J. Z. Jiang, Appl. Phys. Lett. **101**, 092906 (2012).
[8]M. P. Lemeshko, E. S. Nazarenko, A. A. Gonchar, L. A. Reznichenko, T. I. Nedoseykina, A. A. Novakovich, O. Mathon, Y. Joly, and R. V. Vedrinskii, Phys. Rev. B **76**, 134106 (2007).
[9]A. Kodre, J. Tellier, I. Arcon, B. Malic, and M. Kosec, J. Appl. Phys. **105**, 113528 (2009).
[10]D. E. Cox, B. Noheda, G. Shirane, Y. Uesu, K. Fujishiro, and Y. Yamada, Appl. Phys. Lett. **79**, 400 (2001).
[11]M. Hinterstein, J. Rouquette, J. Haines, Ph. Papet, M. Knapp, J. Glaum, and H. Fuess, Phys. Rev. Lett. **107**, 077602 (2011).
[12]B. Ravel and M. Newville, J. Synchrotron Radiat. **12**, 537 (2005).
[13]D. La-Orauttapong, B. Noheda, Z. G. Ye, P. M. Gehring, J. Toulouse, D. E. Cox, and G. Shirane, Phys. Rev. B **65**, 144101 (2002).
[14]W. W. Ge, Y. Ren, J. L. Zhang, C. P. Devreugd, J. F. Li, and D. Viehland, J. Appl. Phys. **111**, 103503 (2012).
[15]K. Wang and J. F. Li, Appl. Phys. Lett. **91**, 262902 (2007).
[16]J. Tellier, B. Malic, B. Dkhil, D. Jenko, J. Cilensek, and M. Kosec, Solid State Sci. **11**, 320–324 (2009).
[17]Y. M. Jin, Y. U. Wang, A. G. Khachaturyan, J. F. Li, and D. Viehland, Phys. Rev. Lett. **91**, 197601 (2003).
[18]M. D. Fontana, G. Métrat, J. L. Servoin, and F. Gervais, J. Phys. C: Solid State Phys. **17**, 483 (1984).
[19]Y. Shiratori, A. Magrez, and C. Pithan, Chem. Phys. Lett. **391**, 288 (2004).
[20]O. Hanske-Petitpierre, Y. Yacoby, J. Mustre de Leon, E. A. Stern, and J. J. Rehr, Phys. Rev. B **44**, 6700 (1991).
[21]Y. Y. Li, Q. H. Liu, T. Yao, Z. Y. Pan, Z. H. Sun, Y. Jiang, H. Zhang, Z. J. Pan, W. S. Yan, and S. Q. Wei, Appl. Phys. Lett. **96**, 091905 (2010).